Modelling of Intracellular Ca^{2+} Alternans and Ca^{2+}-Voltage Coupling in Cardiac Myocytes

Qince Li, Henggui Zhang

Biological Physics Group, University of Manchester, Manchester, UK.

Abstract

In cardiac myocytes, both action potential duration (APD) and mechanical contraction alternans are associated with intracellular Ca^{2+} alternans. The aim of this study is to investigate the interaction between Ca^{2+} and APD alternans by using computer simulations. With a spatially extended (75 elements) model of a single canine ventricular cell, Ca^{2+} and APD alternans were produced either by rapid pacing (3.57 Hz), or by slow pacing (2.5 Hz) with an increased steepness of the relationship between SR Ca^{2+} content and cytoplasimc Ca^{2+} concentration. It is shown that spatially discordant Ca^{2+} alternans is generated when the Ca^{2+}-dependent L-type Ca^{2+} channel inactivation is strong. It tends to be concordant for weak Ca^{2+}-dependent L-type Ca^{2+} channel inactivation.

1. Introduction

Cardiac failure is one of the most common heart diseases associated with fatal cardiac arrhythmias. One of the common symptoms of heart failure is the mechanical alternans, manifested as alternating magnitude of contraction force between large and small [4]. In cardiac tissue, as Ca^{2+} cycling plays the most important role in regulating mechanical contraction, such mechanical alternans may be due to alternation of systolic Ca^{2+} [8]. Another common symptom of heart failure is T-wave alternans on ECG, which makes a possible occurrence of ventricular arrhythmias. As T-wave alternans is associated with the repolarization of ventricular action potentials (APs), it suggests a possible coupling between the Ca^{2+} and the AP alternans.

There are evidences of strong coupling between the membrane potential and the intracellular Ca^{2+} handling [7]. Depolarisation in cell membrane activates the voltage-gated Ca^{2+} channels and brings Ca^{2+} influx to elevate the Ca^{2+} concentration in the cytoplasmic space. The elevated Ca^{2+} concentration triggers the ryanodine receptors (RyRs) to release more Ca^{2+} from the sarcoplasmic reticulum (SR) via a process called calcium-induced calcium release (CICR) [7]. Elevated cytoplasmic Ca^{2+} concentration from both the Ca^{2+} influx and the CICR can affect the L-type Ca^{2+} channels ($I_{Ca,L}$) and the Na^{+}-Ca^{2+} exchanger channels (I_{NaCa}), in turn resulting in a feedback effect on AP. Finally, cytoplasmic Ca^{2+} will be pumped back to the SR or extruded out of the cell via I_{NaCa}. In this process, $I_{Ca,L}$ plays an crucial role in Ca^{2+}-V coupling no matter as the trigger of CICR or the feedback current of $[Ca^{2+}]_i$.

Previous studies have shown that Ca^{2+} and APD alternans can be induced under both fast and slow pacing conditions [1, 2]. However, the complete mechanisms underlying the genesis of systolic Ca^{2+} alternans and its coupling to membrane potential voltage (V) still remain unclear. The aim of this study is to simulate Ca^{2+} and APD alternans under various conditions, from which to elucidate the interaction between them. Moreover, in single cardiac cells, it has been reported that spatially heterogeneous Ca^{2+} alternans can be induced and APD alternans is assumed to be the driving force for determining the pattern of spatial Ca^{2+} alternans [6]. In this study, we also test this hypothesis.

2. Methods and mathematical model

The mathematical model of canine ventricular action potential developed by Shiferaw et al. [5] is used in the study. In the model, a ventricular cell (150 μm) is divided into 75 sarcomeres, which are coupled together via Ca^{2+} diffusion. Each sarcomere is treated as an equivalent functional unit along the longitudinal direction due to T-tubules distribution in the cell. In each element, ionic channels are modeled by equations of Fox et al. [3]. All the parameter values are the same as Ref. [5]. In this model, Ca^{2+}-dependent inactivation of $I_{Ca,L}$ is governed by the parameter γ as shown in the following equation:

$$f_{Ca}^{k,\infty} = \frac{1}{1+\left(c_s^k / \tilde{c}_s\right)^{\gamma}} \quad (1)$$

where c_s^k is the Ca^{2+} concentration in submembrane space; $\tilde{c}_s$ is calcium inactivation threshold.

Steepness of the SR Ca^{2+} release slope is controlled by parameter u in the following equations:

$$\dot{J}_{rel}^{k} = gJ_{Ca}^{k}Q\left(c_j'^{k}\right) - \frac{J_{rel}^{k}}{\tau_r} \quad (2)$$

$$Q\left(c_j'^{k}\right) = \begin{cases} 0 & 0 < c_j'^{k} < 50 \\ c_j'^{k} - 50 & 50 < c_j'^{k} < 110 \\ uc_j'^{k} + s & c_j'^{k} > 110 \end{cases} \quad (3)$$

where c_j' is junctional SR Ca concentration; τ_r is spark life-time.

In simulations, Ca^{2+} and APD alternans are produced either by rapid pacing (3.57 Hz) or slow pacing (2.5 Hz) with an increased parameter u. The mechanism underlying alternans is explored by evaluating the trigger of CICR (i.e. voltage-gated L-type Ca^{2+} current), SR Ca^{2+} content and the relationship between the cytoplasmic Ca^{2+} concentration and the SR Ca^{2+} content during alternans.

3. Results

3.1. Intracellular Ca^{2+} and APD alternans

3.1.1. Alternans induced by fast pacing

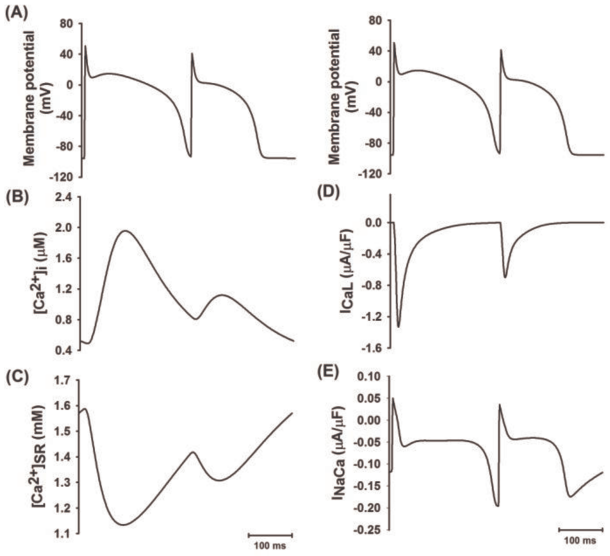

Fig.1. APD and Ca^{2+} alternans induced by fast pacing (3.57 Hz). (A): Action potential. (B): Cytoplasmic Ca^{2+}. (C): SR Ca^{2+} content. (D): L-type Ca^{2+} current. (E): Exchanger current I_{NaCa}.

Fig.1 illustrates the time courses of simulated Ca^{2+} and APs at a pacing rate of 3.57 Hz. Both Ca^{2+} and APD display remarkable alternans under this condition. The peak amplitude of the L-type Ca^{2+} current also alternates dramatically during the two successive beats, which is consistent with previous studies [2]. Alternans of I_{CaL} is due to a short diastolic interval during the fast pacing, that does not allow L-type Ca^{2+} channels to recover from a previous activation, leading to a small L-type Ca^{2+} current in the following beat. Similar alternans is also observed for the SR Ca^{2+} content. Further simulations are performed to test whether the alternans is induced by the varied L-type Ca^{2+} current. By increasing the Ca^{2+}-dependent inactivation rate of $I_{Ca,L}$ which promotes faster inactivation of $I_{Ca,L}$ giving more time for the channel to recover from a previous activation, both the Ca^{2+} and APD alternans are inhibited (not shown here). It is, therefore, the alternation of $I_{Ca,L}$, inducing not only the APD alternans via varying membrane current but also the cytoplasmic Ca^{2+} alternans via influencing CICR, the major factor contributing to alternans under the fast pacing condition.

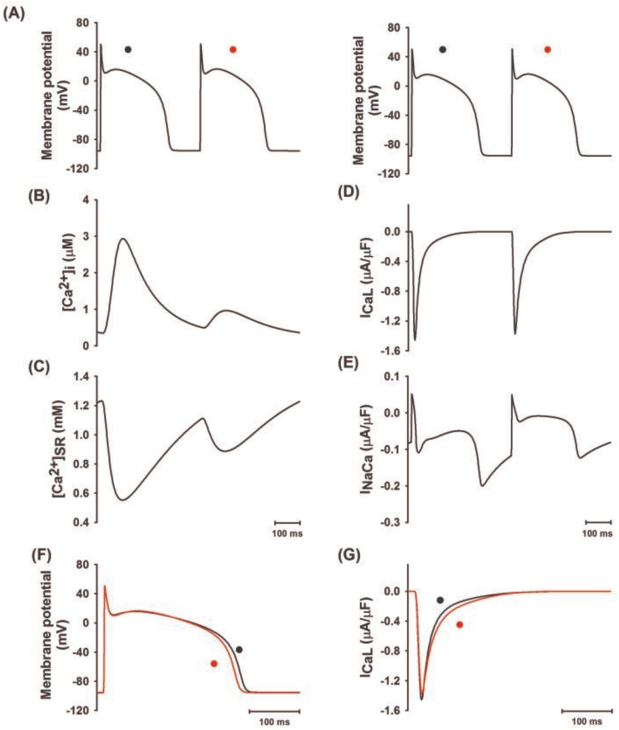

Fig.2. APD and Ca^{2+} alternans induced by increasing the steepness of CICR at slow pacing rate (2.5 Hz). (A): Action potential. (B): Cytoplasmic Ca^{2+}. (C): SR Ca^{2+} content. (D): L-type Ca^{2+} current. (E): Exchanger current I_{NaCa}. (F) and G: Superposition of AP and $I_{Ca,L}$ in two successive beats. Red trace: the beat marked by the red dot in (A). Black trace: the beat marked by the back dot.

3.1.2. Alternans induced by increasing the steepness of CICR

Alternans produced at a slow pacing rate with an increased steepness of Ca^{2+} release is shown in Fig. 2. In this case, amplitude of systolic Ca^{2+} transient varies dramatically in two consecutive pacing cycles. However, the change in APD or amplitude of $I_{Ca,L}$ is very small during alternans. With an increased rate of Ca^{2+}-dependent inactivation, both the alternans, especially the

cytoplasmic Ca^{2+} alternans still remains. Meanwhile, Ca-V coupling becomes negative, with a large-small APD alternans corresponding to a small-large intracellular Ca^{2+} alternans as shown in Fig.3. It suggests that the alternans is due to the varied SR Ca^{2+} release, producing alternating APD via Ca^{2+} dependent membrane currents. Consequentially, the magnitude of $I_{Ca,L}$ alternation is not significant, either the APD alternans. Also, increasing Ca^{2+}-dependent inactivation tends to shorten APD, resulting in a shorter APD though the cytoplasmic Ca^{2+} is higher. This leads to the negative Ca-V coupling.

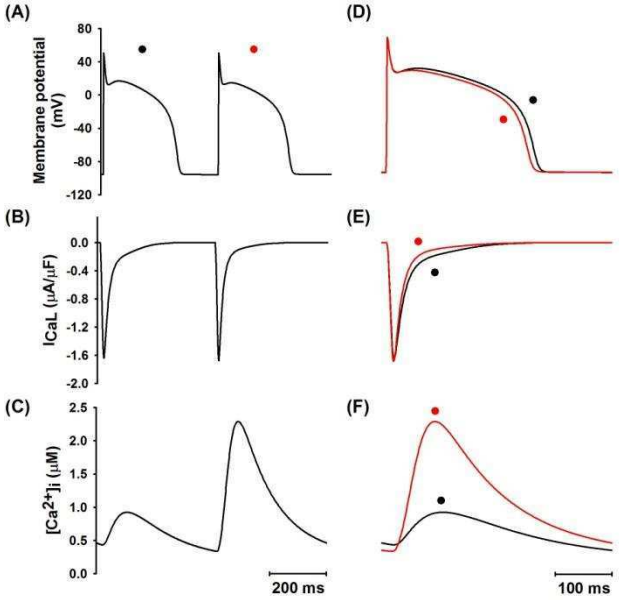

Fig.3. Negative Ca^{2+}-V coupling produced by increasing Ca^{2+}-dependent inactivation of $I_{Ca,L}$. (A): Action potential. (B): $I_{Ca,L}$. (C): Cytoplasmic Ca^{2+}. (D), (E) and (F) are corresponding superposition graph in two successive beats.

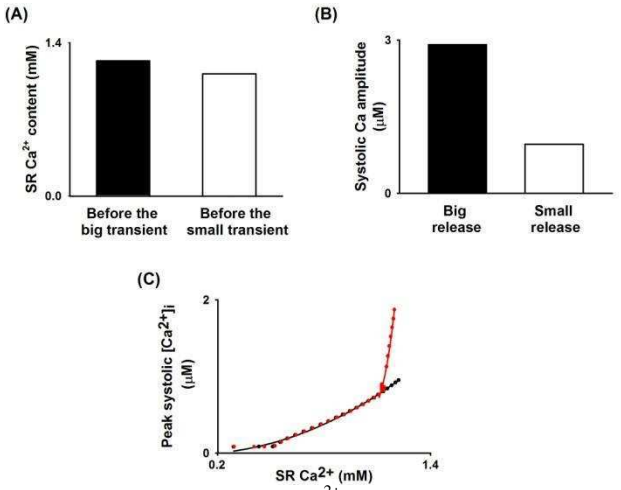

Fig.4. Relationship between $[Ca^{2+}]_i$ and the SR content during alternans. (A): SR Ca^{2+} content. (B): Systolic Ca^{2+} amplitude. (C): relationship of $[Ca^{2+}]_i$ and the SR content. Black circles: control condition. Red circles: alternans condition.

The relationship between the SR Ca^{2+} content and peak systolic Ca^{2+} during the alterans is explored. Results are shown in Fig.4. SR Ca^{2+} content before a large Ca^{2+} transient is slightly higher than that before a small transient. The relationship between SR Ca^{2+} content and systolic Ca^{2+} is smooth under control condition, but becomes much steeper when alternans begins to emerge (The curves is fitted by the formula [systolic Ca^{2+}] = a + b×[SR Ca^{2+}]^n; control condition: n = 2.1; alternans condition: n = 16.3.). This steep relationship gives a rise of a large change of systolic Ca^{2+} amplitude in response to a small variation in the SR Ca^{2+} content. This suggests that the varied CICR is the key factor responsible for the intracellular Ca^{2+} alternans at slow pacing rate.

3.2. Spatially concordant and discordant alternans

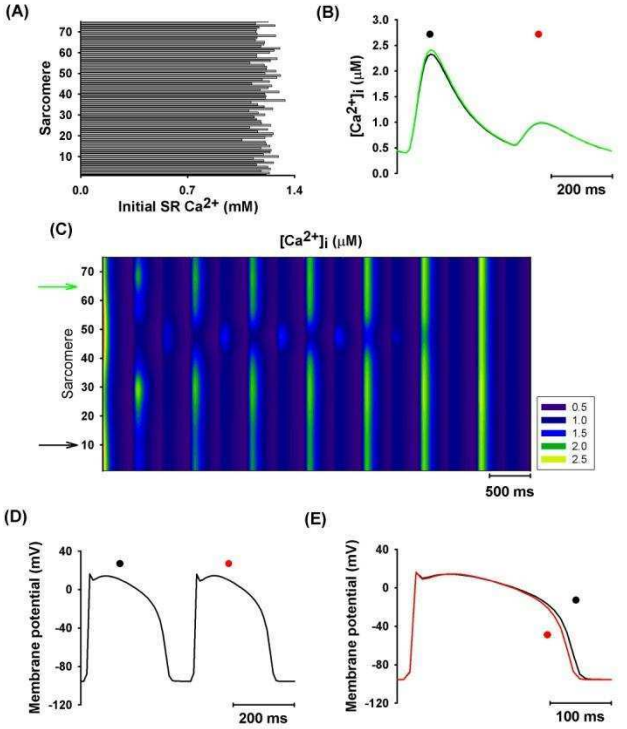

Fig.5. Concordant Ca^{2+} alternans induced at fast pacing rate. (A): Initial distribution of SR content. (B): Traces of $[Ca^{2+}]_i$ alternans corresponding to the region marked by the arrow in panel C. (C): Line scan image of cytoplasmic Ca^{2+}. (D): AP traces. (E): Superposition of APs in two successive beats.

Spatial Ca^{2+} alternans is examined in the 75 elements of the cell model at fast pacing condition (2.86 Hz). In the model, a Gaussian distribution with a 20% deviation of the average value is applied for the initial values of the SR Ca^{2+} content as shown in Fig. 5A. This results in out-of-phase Ca^{2+} alternans in the 75 elements. But it only sustains for the first few cycles, and gradually evolves into in-phase alternans throughout the whole cell. Under

the fast pacing condition, APD alternans is induced by incompletely recovery of membrane I_{CaL} current as discussed above. It tends to synchronize the phase of intracellular Ca^{2+} alternans via L-type Ca^{2+} current. Also, the large Ca^{2+} transient during alternans could produce strong Ca^{2+} diffusion, which tends to reduce the heterogeneity of Ca^{2+} distribution. Both of these effects drive Ca^{2+} alternans to be in phase throughout the cell.

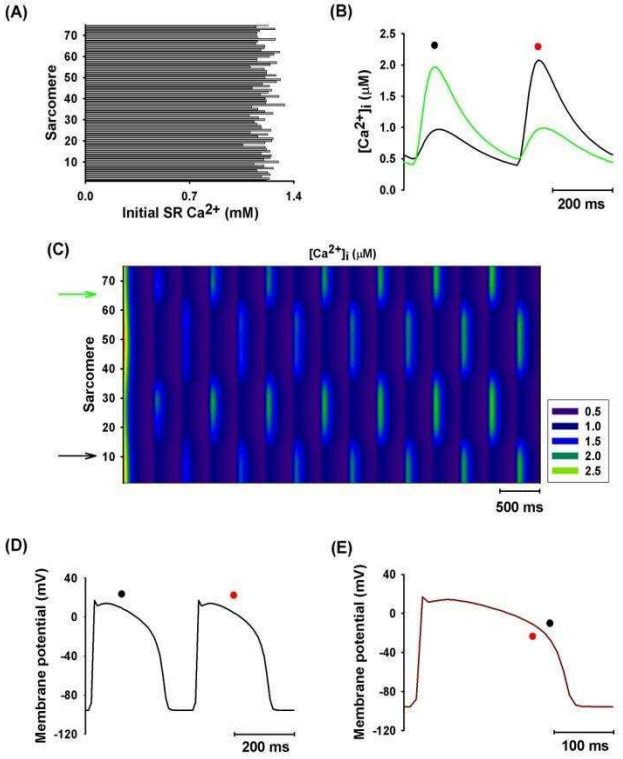

Fig.6. Spatiotemporal evolution of discordant Ca^{2+} alternans. (A): Initial distribution of SR content. (B): Traces of $[Ca^{2+}]_i$ alternans corresponding to the region marked by the arrow in panel C. (C): Line scan image of cytoplasmic Ca^{2+}. (D): AP traces. (E): Superposition of APs in two successive beats.

Fig. 6 shows the spatially heterogeneous Ca^{2+} alternans produced with the same initial condition, but with an increased Ca^{2+}-dependent inactivation of $I_{Ca,L}$. As increased Ca^{2+}-dependent inactivation gives more time for $I_{Ca,L}$ to recover, it thus reduces APD alternans (Fig. 6E). Therefore, local Ca^{2+} alternans tends to remain out-of-phase without a driving force reducing the heterogeneity from APD alternans. Meanwhile, an increased Ca^{2+}-dependent inactivation enhances local coupling of Ca^{2+} and $I_{Ca,L}$, which increases heterogeneity of global distribution of Ca^{2+} transient. Moreover, spatially heterogeneous Ca^{2+} alternans also can be induced while APD alternant presents (results are not shown here). Therefore, the spatial pattern of Ca^{2+} alternans is determined by the interaction between global AP and local Ca^{2+} dynamics.

4. Conclusion

In this study, we present different mechanisms underlying the genesis of Ca^{2+} and APD alternans induced at both fast and slow pacing. It is shown that APD and Ca^{2+} alternans are correlated with each other via membrane Ca^{2+}-dependent channels. The interaction between them is associated with the phase of Ca^{2+}-V coupling (positive or negative) during alternans. Such an interaction plays an important role in determining the spatial pattern of cytoplasmic Ca^{2+} alternans, either concordant or discordant throughout the cell.

Acknowledgement

The work is supported by project grants from the BBSRC, BHF UK and ORS studentship.

References

[1] Mary E. Díaz, Stephen C. O'Neill and David A. Eisner. Sarcoplasmic reticulum calcium content fluctuation is the key to cardiac alternans. Circ. Res. 2004; 94:650-656.

[2] Hüser, J., Wang, Y.G., Sheehan, K.A., Cifuentes, F., Lipsius, S.L., Blatter, L.A.. Functional coupling between glycolysis and excitation-contraction coupling underlies alternans in cat heart cells. The Journal of physiology 2000; 524.3:795-806.

[3] Fox, J.J., McHarg, J.L., Gilmour Jr., R.F.. Ionic mechanism of electrical alternans. American Journal of Physiology - Heart and Circulatory Physiology 2001; 282:H516-H530.

[4] Tao, T., O'Neill, S.C., Diaz, M.E., Li, Y.T., Eisner, D.A., Zhang, H.. Alternans of cardiac calcium cycling in a cluster of ryanodine receptors: A simulation study. American Journal of Physiology - Heart and Circulatory Physiology 2008; 295: H595-H609.

[5] Shiferaw, Y., Karma, A.. Turing instability mediated by voltage and calcium diffusion in paced cardiac cells. Proceedings of the National Academy of Sciences of the United States of America 2006; 103(15): 5670-5675.

[6] Aistrup, G.L., Shiferaw, Y., Kapur, S., Kadish, A.H., Wasserstrom, J.A.. Mechanisms underlying the formation and dynamics of subcellular calcium alternans in the intact rat heart. Circulation Research 2009; 104 (5): 639-649.

[7] Bers, D.M.. Cardiac excitation-contraction coupling. Nature 2002; 415 (6868):198-205.

[8] Lab, M.J., Lee, J.A.. Changes in intracellular calcium during mechanical alternans in isolated ferret ventricular muscle. Circulation Research 1990; 66 (3):585-595.

Address for correspondence

Henggui Zhang
Room 3.07, Shuster building
The School of Physics and Astronomy
The University of Manchester, Oxford Road
Manchester, M13 9PL, UK
E-mail: H.Zhang-3@manchester.ac.uk